J Therm Anal Calorim (2015) 122:235–240
DOI 10.1007/s10973-015-4680-3

Deacetylation-induced changes in thermal properties of *Sterculia urens* gum

Niranjan Patra[1] · Lucy Vojtová[2] · Lenka Martinová[1]

Received: 12 August 2014 / Accepted: 28 March 2015 / Published online: 16 April 2015
© Akadémiai Kiadó, Budapest, Hungary 2015

Abstract A quantitative measurement of degree of deacetylation of *Sterculia urens* gum and its effect on the thermal properties changes is presented in this study. *Sterculia urens* gum was deacetylated at varying deacetylation reaction temperature and time. The acetyl group is replaced by hydroxyl which leads to better solubility of the *sterculia* gum in water. Thermal properties were characterized using differential scanning calorimetry and thermogravimetric analysis. DSC analysis reveals that after the deacetylation, the glass transition temperature appears at around 60 °C of the *S. urens* gum. After deacetylation, the TG degradation clearly shows three different peaks. Deacetylation reaction temperature plays the major role in the thermal stability and structure of the *S. urens* gum.

Keywords *Sterculia urens* · Deacetylation · Thermal properties · TG · DSC

Introduction

Recently, there is an immense interest in using the naturally available tree gum polysaccharides because of their low cost, easy availability and non-toxic characteristics to be used in industry, biomedical, food and cosmetics. Tree wound exudates gum of natural acid polysaccharide which has attracted huge attention among researcher because of their immense potential application in food industry, biomedical as well as material science [1–8]. Natural anionic acid polysaccharides are inexpensive, easily available, non-toxic, biodegradable materials which exhibit peculiar physicochemical properties and applications [6, 9, 10]. Gum karaya (GK) is a partially acetylated natural polysaccharide having branched structure with high molecular mass of 16×10^6 Da and grouped under substituted rhamnogalacturonoglycan (pectic)-type tree gums. GK contains neutral sugars of 13–26 % of D-galactose and 15–30 % of L-rhamnose and acidic sugars like D-glucuronic acid and galacturonic acid which is higher compared to other tree gum exudates [4]. Karaya gum contains 8 % acetyl group. However, protein content of karaya is lesser than other exudates gum. GK is commonly used for food and non-food applications due to its acid stability, high viscosity and suspension properties [6].

It is essential to know the thermal properties of the food hydrocolloids for better product development, quality control, design and evaluation of the process. The objective of the present work is to study the effect of deacetylation on the thermal properties of the *Sterculia urens*. Deacetylation was carried out at different reaction time and temperature. From this, we got different degree of deacetylation. The thermal properties changes on *S. urens* upon different degree of deacetylation were studied.

Experimental

Sterculia urens (gum karaya) obtained from Sigma-Aldrich company was used in the experiment. Double-distilled water was used for dissolving *S. urens* gum. Ammonia

✉ Niranjan Patra
patraji@gmail.com

[1] Centre for Nanomaterials, Advanced Technologies and Innovation, Technical University of Liberec, Studentská 1402/2, 461 17 Liberec, Czech Republic

[2] CEITEC – Central European Institute of Technology, Brno University of Technology, Technická 3058/10, 616 00 Brno, Czech Republic

solution (25 % in H_2O) from Sigma-Aldrich was used to maintain the pH for deacetylation reaction. For the deacetylation reaction, *S. urens* of 1 mass% was taken in a glass beaker with 100 mL of water. The gum solution was stirred with the help of a magnetic stirrer. Deacetylation was carried out at a constant pH of 10. Estimated amount of ammonia solution was used to maintain the pH at 10. The deacetylation reaction was carried out at different temperature of 30, 40, 50 and 60 °C and time 6, 17 and 30 h in order to see the nature and degree of deacetylation. After the deacetylation reaction, the solution was neutralized by adding small amount of diluted hydrochloric acid. The solution was filtered using a sintered filter (Sintered Glass Buchner Funnel) to remove any foreign particles. Then, the *sterculia* gum solution was precipitated and centrifuged using ethanol, and the precipitate was dried at a temperature of 40 °C using a centrifuged air dryer for 24 h. The dried deacetylated gum was later crushed to powder in a ceramic mortar. The original as received *S. urens* powder is designated as PGK. This deacetylated sample was designated as DGK sample.

FT-IR spectra of pristine and deacetylated *sterculia* gum were acquired in the range of 600–4000 cm^{-1}, using a Bruker VERTEX 80/80v FTIR spectrometer. The samples were analyzed directly on an attenuated total reflection (ATR) platform with diamond crystal. For optimal signal-to-noise ratio, 32 scans were averaged per sample spectrum and apodized by Blackmann–Harish three-term apodization correction functions to avoid interference for the Fourier transformation. All the spectra were baseline-corrected by second-order polynomial and were normalized thereafter. The degree of deacetylation was calculated from the ratio of absorbance band of acetyl group of pristine to the deacetylated *S. urens* at 1740 cm^{-1} with the reference band of 2940 and 1040 cm^{-1}. This particular band is chosen since this band represents the acetyl group.

DSC measurements of pristine and deacetylated *sterculia* were carried out on a DSC 204 F1 Phoenix (Germany), operating between 0 and 500 °C with a ramping rate of 10 °C min^{-1}, operating in a N_2 atmosphere at a flow rate of 20 mL min^{-1}. ~5 mg of sample crimped in an aluminum pans was used for the experiment. The DSC instrument was calibrated based on the melt onset and heat of fusion of indium at 156.6 °C and 28.4 J g^{-1} as the standard materials.

TG measurements were carried out on a TA instrument (TA Q500) apparatus working in N_2 atmosphere between 30 and 900 °C, with a heating rate of 10 °C min^{-1}. The TG measurement was also carried out in air atmosphere. From the TG traces, differential thermogravimetric (DTG) plots were calculated as the first derivative of the TG curves. The amount of sample was approximately 10 mg in all the TG measurements.

Results and discussion

Figures 1 and 2 show the normalized FT-IR absorption spectral band of PGK and DGK at different deacetylation temperatures and time in order to quantify the degree of deacetylation. The major bands observed for *S. urens* gum corresponding to vibrations of characteristic groups. The broad band at 3370 cm^{-1} corresponds to O–H stretching band of hydroxyl group and N–H stretching band of amide group of galactopyranose and glucopyranose ring; 1725 cm^{-1} C=O due to the stretching vibration; 1595 cm^{-1} to the C=C band; that of 1417 cm^{-1} to the CO_{2-} symmetric stretching and 1371 cm^{-1} represents the C–H deformation. The band at 1244 cm^{-1} is due to the C–O stretching vibration. From Fig. 3a, b, the degree of deacetylation is calculated for both deacetylation by

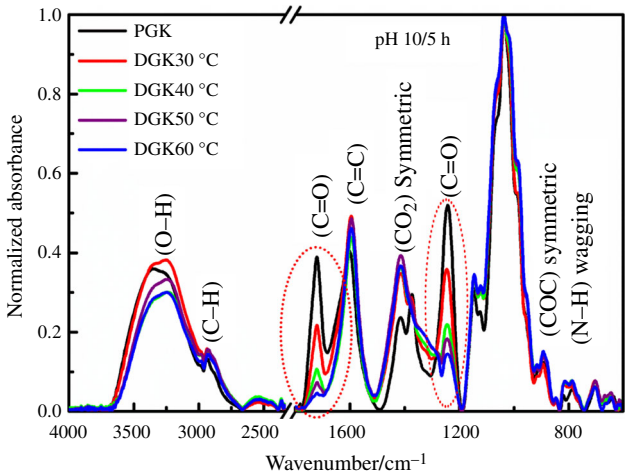

Fig. 1 Normalized FT-IR spectra of PGK and DGK at different temperatures at pH 10 for 5 h

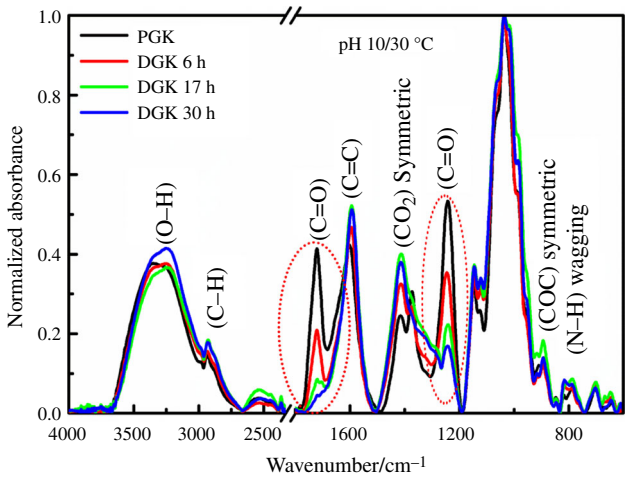

Fig. 2 Normalized FT-IR spectra of PGK and DGK at different time of 6, 17 and 30 h at 30 °C

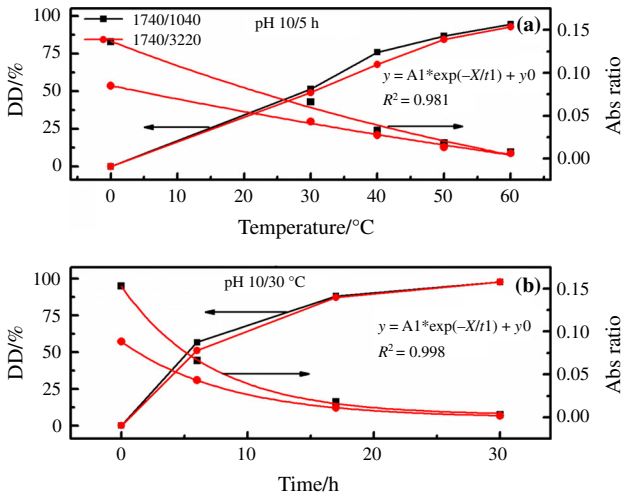

Fig. 3 Degree of deacetylation DD/% of *Sterculia urens* gum calculated from the ratio of absorbance peak of acetyl band with reference band of hydroxyl **a** deacetylation at different temperatures; b deacetylation at different times

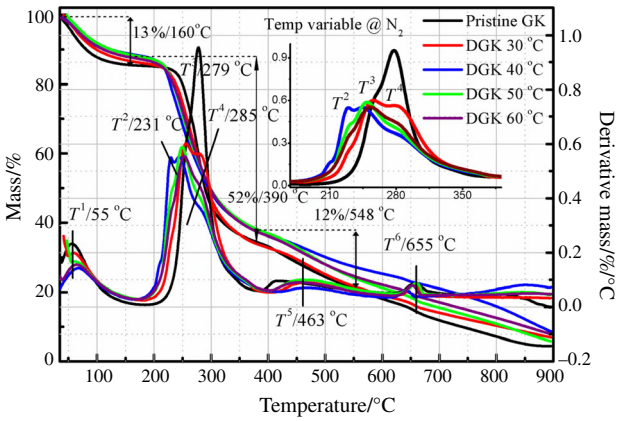

Fig. 4 TG–DTG of PGK and DGK deacetylated at different temperatures. *Inset* zoomed plot of the major DTG degradation peak

varying temperature and time. The maximum degree of deacetylation (93 %) is observed for the highest reaction temperature of 60 °C and lowest of 57 % for reaction temperature of 30 °C. However, high reaction temperature shows instability of the solution which leads to chemical degradation showing a darker in color of *sterculia* solution. Similarly, for the reaction with time variables, the maximum degree of deacetylation (97 %) was observed for 30 h of deacetylation and minimum of 55 % for 6 h. In deacetylation reaction (Fig. 1) at high temperatures, the O–H stretching band becomes narrower than the pristine and deacetylated at 30 °C because of the weak intermolecular interaction. Again the intensity of the O–H stretching band also decreases with increasing temperature of deacetylation. For deacetylation at different time in Fig. 2, the hydroxyl peak is unaffected with the time. The ratio of absorbance peak in Fig. 1 (1725/1595) increases with increasing temperature by increasing the intensity of the 1595 band. The ratio of the 1725/1595 band is highest for deacetylation in 60 °C which is 1:11.5. The band intensity ratio of pristine PGK is 1:1. In case of deacetylation with time variation, the maximum band intensity ratio for 30 h deacetylation is 1:12.7. There is no change in any other band of the *sterculia* gum.

Thermogravimetric analysis has been used as an excellent tool to investigate the decomposition, stability and purity of materials by many investigators [8, 11–17]. Figure 4 shows the TG and DTG curve along with the insets of zoomed DTG curve of the major degradation step of pristine, and deacetylated *sterculia* at different temperature in nitrogen atmosphere is presented. From the TG curve, approximately 15 % for the PGK and 13 % mass loss for the DGK are observed at temperature up to 160 °C which is due to the high water-absorbing capacity of the tree gum polysaccharides. The maximum mass loss for the absorbed water occurs at temperature T^1/55 °C which is clear in the DTG curve. The major degradation of 52 % occurs from 160 to 390 °C. From the DTG curve, we can see that for the deacetylated samples this major degradation occurs in three steps which are represented in the DTG as a shoulder plot that is T^2, T^3 and T^4 at around 231, 256 and 284 °C, respectively. However, for the PGK, the major degradation occurs only in two steps. In case of the deacetylated sample, the degradation DTG plot is broader than the PGK which is sharper. The major mass loss is due to the degradation of sugars. After the major degradation step, there is another mass loss occurs which is represented in the DTG curve at T^5 at 463 °C and end at 548 °C. This 12 % mass loss is believed to be due to the elemental composition like calcium and magnesium which is present in the original samples. The small mass loss at T^6/655 °C is due to the combustion of the small amorphous carbon formed from the polysaccharides.

Figure 5 presents the TG and DTG analysis curve in air atmosphere of PGK and DGK at different reaction temperature, respectively. The degradation of *sterculia* in air atmosphere occurs in several steps. The first mass loss of around 20 % for PGK and around 13–15 % for the DGK is due to the absorbed water or moisture from the atmosphere which ends at temperature at 170 °C. The maximum mass loss for the water occurs at around 58 °C which is represented in the DTG plot at T^1. The major mass loss for PGK and DGK occurs from temperature 170 to 375 °C which is 15° less than in nitrogen atmosphere. Here, the maximum mass loss for the major degradation step is 53 %. In case of air atmosphere, the PGK shows two-shoulder peaks of the major degradation step which is at 255 and 275 °C, whereas in case of the DGK there is three-shoulder peak which appears at 230, 254 and 279 °C represented, as T^2, T^3 and T^4 in DTG plot, respectively. The interesting things

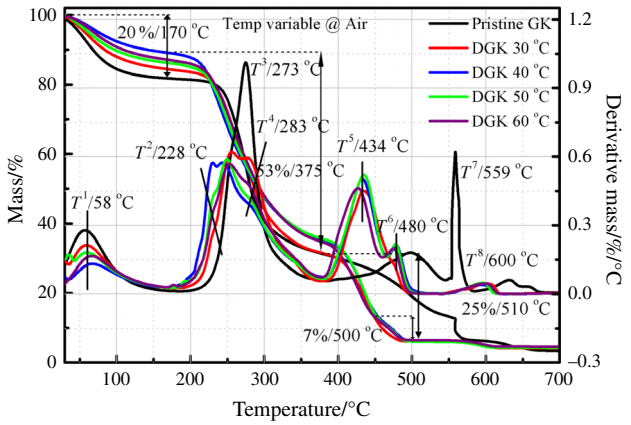

Fig. 5 TG and DTG done in air atmosphere of PGK and DGK deacetylated at different temperature

to note in this major degradation plot is that for the pristine *sterculia*, the major DTG degradation plot is higher in height and narrower, where for the DGK it is smaller and broader. In DTG plot, the T^2 peak of the DGK at 40 °C is shifted to lower temperature compare to the other samples. Again if we see closely, we can see that the T^3 and T^4 peaks of the DGK at 30 °C (red curve) are more or less similar in height, whereas the T^4 peak height decreases as the deacetylation reaction temperature increases. After the major degradation step, another mass loss occurs. For the PGK, this mass loss is represented clearly in the DTG peak at T^5 at 498 °C, whereas for the deacetylated samples this T^5 peak is shifted to left at temperatures of both 434 and 480 °C for 25 % mass loss. The degradation step occurs at 560 °C at T^7 for PGK where as it is absent in the DGK. The final small mass loss occurs at 632 °C for PGK and 600 °C for DGK.

Figure 6 shows the thermogravimetric and differential thermogravimetry analysis graph done in nitrogen atmosphere of pristine and *sterculia* deacetylated at 30 °C

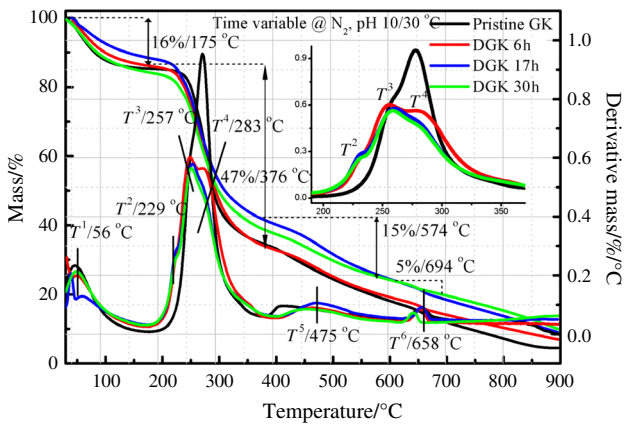

Fig. 6 TG and DTG curve done in nitrogen atmosphere of PGK and *sterculia* deacetylated at different time. *Inset* zoomed graph of the major DTG degradation peak

reaction temperature at pH 10 for different time interval of 6, 17 and 30 h, respectively. The first mass loss of approximately 16 % which is due to the absorbed water occurs up to temperature of 175 °C with the maximum mass loss occurs at T^1 at 56 °C. In case of *sterculia* deacetylated at different temperature, this mass loss occurs up to a temperature of 160 °C. The major degradation steps from 175 to 376 °C with a mass loss of 47 %. From the DTG plot, it is very clear that the major degradation step is having three-shoulder peak which is zoomed and represented in T^2, T^3 and T^4 at 229, 253 and 282 °C, respectively. One important point we note here that at different time for deacetylation, these three peaks at T^2, T^3 and T^4 are very similar for all the deacetylation time interval whereas in case of deacetylation for different temperature, the T^2, T^3 and T^4 peaks shifted to little lower temperature as the reaction temperature increases. The third mass loss curve occurs from 382 to 575 °C with a mass loss of 15 % which is little higher in case of pristine and the sample deacetylated for 6 h. The maximum mass loss T^5 occurs at 475 °C. The mass loss of 5 % at 694 °C with maximum loss T^6 at 658 °C.

Figure 7 shows the TG–DTG curve done in air atmosphere of PGK and *sterculia* deacetylated at varying time with constant pH and temperature, respectively. The initial mass loss of 20 % occurs for the pristine sample, and 16 % for the deacetylated sample is due to the absorbed water from the environment. The maximum mass loss occurs at around T^1 58 °C from the DTG plot. The major degradation in case of DGK at different time occurs from 175 to 370 °C with 46 %. However, we can see that in this degradation range, the mass loss of deacetylated samples for 17 and 30 h is a little lesser than the PGK and DGK for 6 h. From the DTG plot, there is also three-shoulder peak from the major degradation zone that is T^2, T^3 and T^4 at 230, 255 and 275 °C. From the nature of T^2, T^3 and T^4, it is clear that the

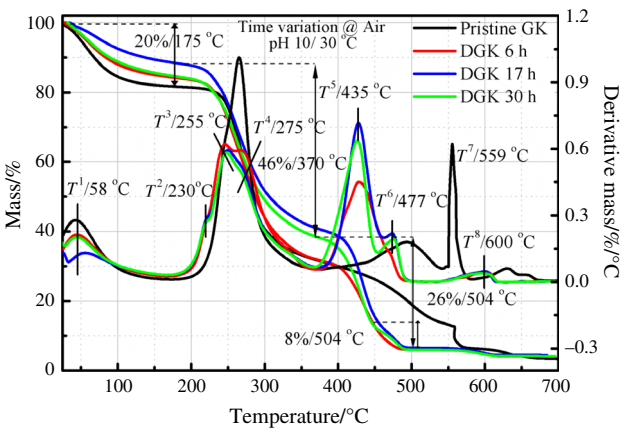

Fig. 7 TG–DTG of PGK and *sterculia* deacetylated at different time in air atmosphere

nature of the degradation for deacetylated samples at constant pH and temperature with varying time is almost the same. If we correlate the result of Fig. 5 with Fig. 7, it may be deduced that the thermal stability of the *sterculia* decreases substantially when we increases the deacetylation temperatures, whereas at constant temperature deacetylation it was the same for all the time interval deacetylation. The next step of degradation in Fig. 7 occurs from 370 to 505 °C with two DTG peak at T^5/435 °C and T^6/477 °C, whereas in case of PGK it was broader and shifted to higher temperatures with DTG peak at 500 °C. There is a sharp peak appears for the pristine sample at T^7/559 °C, whereas for DGK the peak T^8 is smaller and broader. The T^8 DTG peak for the DGK is at 600 °C. The sharp peak T^7 is absent in the deacetylated samples.

Differential scanning calorimetry has been used extensively to investigate the thermal properties of materials [18]. Figure 8 illustrates the DSC heating curve of PGK and DGK at different temperatures, i.e., 30, 40, 50 and 60 °C along with the conversion curve for both endothermic and exothermic peaks, respectively. For all experiment, the mass of the DSC sample is approximately same. In order to see the consistency and reproducibility, three measurements for each sample were carried out. In the inset of Fig. 8, the zoomed curve of the entire curve from 40 to 80 °C is presented. The small increase in the baseline is believed to be the glass transition temperature of *sterculia* samples after deacetylation. The glass transition T_g of the sample is not found for the PGK at the experimental DSC temperature ranges taken. The T_g shown in DGK is due to the degree of branching and intermolecular interaction in the *S. urens* chain. The broad endothermic peak is observed for PGK at around 122 °C which is 20 °C more for the DGK which is due to the breaking of the long nucleotides and removal of the hydrogen bound water. The DSC values are tabulated in Table 1. This peak is broader which signifies a bigger

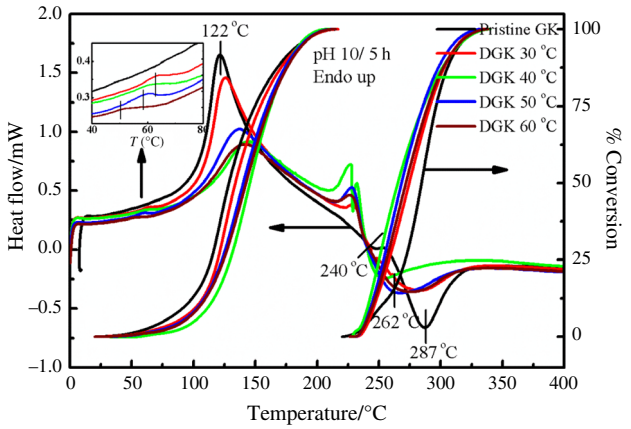

Fig. 8 DSC of PGK and DGK at different temperatures along with the percentage amount of the sample that has converted at exothermic and endothermic zone of each sample

Table 1 DSC results of PGK and DGK at different reaction temperature and time

Sample	Peak/°C		Area under peak/mJ		ΔH/J g^{-1}	
	Endo	Exo	Endo	Exo	Endo	Exo
Sterculia Urens/temperature						
PGK	121	287	435	−173	83.6	33.2
DGK30	126	276	374	−183	73.3	35.8
DGK40	144	250	174	−219	32.2	40.5
DGK50	137	262	264	−234	49.8	44.1
DGK60	140	263	224	−210	43	40.3
Sterculia Urens/time						
PGK	121	287	435	−173	83.6	33.2
DGK6	126	276	374	−183	73.3	35.8
DGK17	137	284	229	−264	40.8	47.1
DGK30	125	285	385	−236	66.3	40.6

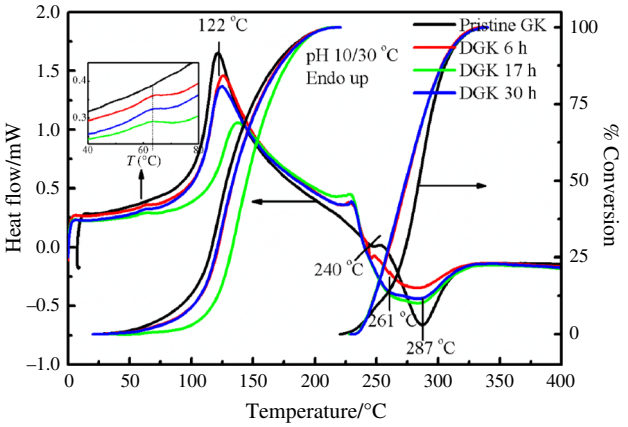

Fig. 9 DSC of PGK and DGK at different time along with the percentage amount of the sample that has converted at exothermic and endothermic peak of each sample

crystallite size distribution. From Table 1, the endothermic peak appears in 122 °C for the PGK and the sample deacetylated at 30 °C whereas the *sterculia* deacetylated at 40, 50 and 60 °C, and this peak was shifted to a higher temperature up to 20 °C more because of the dangling of the polymer chain which occurs due to agitation during the deacetylation reaction. After the broad endothermic peak, an exothermic peak shows the scissions of the chains leading to degradation of the polysaccharide mainly sugars. There is two exothermic peak of *sterculia*, indicating the degradation of various sugars and needs higher energy for breaking the bonds. While for the DGK, the exothermic degradation peak of *sterculia* shows three-shoulder peak in the major degradation steps. From Table 1, it is also clear that for the *sterculia* deacetylated at different reaction temperatures, the ΔH values are more than the pristine samples.

Figure 9 shows the DSC heating scans of PGK and DGK for different time with constant temperature and pH

along with the conversion curve for both endothermic and exothermic peaks, respectively. In the inset, the zoomed image from 40 to 80 °C is also represented in order to see clearly the small change which is believed to be the T_g of the sample. For all DGK sample for different time, the T_g is similar at one temperature. The next broad and big endothermic peak at 121 °C for PGK is due to the removal of the bounded water in the polysaccharide nucleotides. However, there is a little change of endothermic peak for the deacetyl sample which is presented in Table 1. The exothermic peak for the DGK sample for different time shows the same nature with three-shoulder peak at 240, 261 and 287 °C, respectively. From Table 1, it is clear that the enthalpy varies for the different deacetylation reaction time. The maximum enthalpy values for the PGK sample are 33 J g^{-1} for the exothermic peak, whereas it increases a little for the other sample to 35, 47 and 40 J g^{-1}.

In DSC the enthalpy, peak temperature and the peak area are the most important parameter in order to study the thermal behavior of the material. This thermal behavior is also to be analyzed by conversion curve of DSC of the respective peak area. The conversion curve mainly indicated the % of crystals that has converted. The percent conversion α (T) is calculated from the heat flow curve of endo and exo peak:

$$\alpha(T) = \frac{\Delta H_{\text{part}}}{\Delta H_{\text{tot}}} \times 100\,\% = \frac{\int_{T_0}^{T} \emptyset(T')\mathrm{d}T'}{\int_{T_o}^{T_i} \emptyset(T')\mathrm{d}T'} \times 100\,\%$$

where T_0 is the lower temperature limit of the peak evaluation and T' is the upper temperature limit. The partial area of the peak from the temperature T_0 to the actual temperature T' is H_{part}. The total area of the peak is H_{tot}.

From the conversion curve, one can see that for the endothermic conversion curve the reaction is slower till about 60 °C, but once it reached to about 70 °C the reaction becomes significantly faster.

Conclusions

Glass transition temperature appears after deacetylation due to the strong intermolecular junction formed in the polysaccharide chains due to the hydrogen bonding of rhamnose. The degradation behavior of *sterculia* changed after the deacetylation showing a broad exothermic behavior with three overlapping peak for rhamnose, galactose and the uronic acid content.

Acknowledgements The research reported in this paper was supported in part by the Project OP VaVpI Centre for Nanomaterials, Advanced Technologies and Innovation CZ.1.05/2.1.00/01.0005 and by the Project Development of Research Teams of R&D Projects at the Technical university of Liberec CZ.1.07/2.3.00/30.0024.

References

1. Chen J, Jo S, Park K. Polysaccharide hydrogels for protein drug delivery. Carbohydr Polym. 1995;28:69–76.
2. de Brito ACF, Sierakowski MR, Reicher F, Feitosa JPA, de Paula RCM. Dynamic rheological study of sterculia striata and karaya polysaccharides in aqueous solution. Food Hydrocoll. 2005;19:861–7.
3. De Paula RCM, Rodrigues JF. Composition and rheological properties of cashew tree gum, the exudate polysaccharide from *Anacardium occidentale* L. Carbohydr Polym. 1995;26:177–81.
4. Le Cerf D, Irinei F, Muller G. Solution properties of gum exudates from *Sterculia urens* (karaya gum). Carbohydr Polym. 1990;13:375–86.
5. Silva DA, Brito ACF, de Paula RCM, Feitosa JPA, Paula HCB. Effect of mono and divalent salts on gelation of native, Na and deacetylated sterculia striata and *Sterculia urens* polysaccharide gels. Carbohydr Polym. 2003;54:229–36.
6. Verbeken D, Dierckx S, Dewettinck K. Exudate gums: occurrence, production, and applications. Appl Microbiol Biotechnol. 2003;63:10–21.
7. Patra N, Jayaseelan DD, Lee WE. Synthesis of biopolymer-derived zirconium carbide powder by facile one-pot reaction. J Am Ceram Soc. 2015;98:71–7
8. Patra N, Martinová L, Stuchlik M, Černík M. Structure–property relationships in *Sterculia urens*/polyvinyl alcohol electrospun composite nanofibres. Carbohydr Polym. 2014;120:69–73.
9. Vinod VTP, Sashidhar RB. Surface morphology, chemical and structural assignment of gum Kondagogu (Cochlospermum gossypium DC.): an exudate tree gum of India. Indian J Nat Prod Resour. 2010;1:181–92.
10. Vinod VTP, Sashidhar RB, Sarma VUM. Vijaya Saradhi UVR. Compositional analysis and rheological properties of gum kondagogu (Cochlospermum gossypium): a tree gum from India. J Agric Food Chem. 2008;56:2199–207.
11. Patra N, Hladik J, Martinova L. Investigating the thermal properties of polyethylene plasma modified by using unconventional chemical vapors. J Therm Anal Calorim. 2014;117:229–34.
12. Patra N, Hladik J, Pavlatová M, Militký J, Martinová L. Investigation of plasma-induced thermal, structural and wettability changes on low density polyethylene powder. Polym Degrad Stab. 2013;98:1489–94.
13. Patra N, Jayaseelan DD, Lee WE. Synthesis of biopolymer-derived zirconium carbide powder by facile one-pot reaction. J Am Ceram Soc. 2015;98:71–7.
14. Patra N, Salerno M, Cozzoli PD, Athanassiou A. Surfactant-induced thermomechanical and morphological changes in TiO_2-polystyrene nanocomposites. J Coll Interface Sci. 2013;405:103–8.
15. Patra N, Salerno M, Cozzoli PD, Barone AC, Ceseracciu L, Pignatelli F, et al. Thermal and mechanical characterization of poly(methyl methacrylate) nanocomposites filled with TiO_2 nanorods. Compos B Eng. 2012;43:3114–9.
16. Mishra N, Patra N, Pandey S, Salerno M, Sharon M, Sharon M. Taguchi method optimization of wax production from pyrolysis of waste polypropylene. J Therm Anal Calorim. 2014;117:885–92.
17. Patra N, Salerno M, Malerba M, Cozzoli PD, Athanassia A. Improvement of thermal stability of poly(methyl methacrylate) by incorporation of colloidal TiO_2 nanorods. Polym Degrad Stab. 2011;96:1377–81.
18. Patra N, Barone AC, Salerno M. Solvent effects on the thermal and mechanical properties of poly(methyl methacrylate) casted from concentrated solutions. Adv Polym Technol. 2011;30:12–20.